Research Article Vol. 9, No. 5 / May 2022 / Optica 565

Exotic interactions mediated by a non-Hermitian photonic bath

Federico Roccati,[1,*] Salvatore Lorenzo,[1] Giuseppe Calajò,[2] G. Massimo Palma,[1,3] Angelo Carollo,[1,4] and Francesco Ciccarello[1,3]

[1]Dipartimento di Fisica e Chimica – Emilio Segrè, Università degli Studi di Palermo, via Archirafi 36, I-90123 Palermo, Italy
[2]ICFO-Institut de Ciencies Fotoniques, The Barcelona Institute of Science and Technology, 08860 Castelldefels (Barcelona), Spain
[3]NEST, Istituto Nanoscienze-CNR, Piazza S. Silvestro 12, 56127 Pisa, Italy
[4]Radiophysics Department, National Research Lobachevsky State University of Nizhni Novgorod, 23 Gagarin Avenue, Nizhni Novgorod 603950, Russia
*Corresponding author: federico.roccati@unipa.it

Received 23 September 2021; revised 13 February 2022; accepted 22 March 2022; published 18 May 2022

Photon-mediated interaction between quantum emitters in engineered photonic baths is an emerging area of quantum optics. At the same time, non-Hermitian (NH) physics is currently thriving, spurred by the exciting possibility to access new physics in systems ruled by non-trivial NH Hamiltonians—in particular, photonic lattices—which can challenge longstanding tenets such as the Bloch theory of bands. Here, we combine these two fields and study the exotic interaction between emitters mediated by the photonic modes of a lossy photonic lattice described by a NH Hamiltonian. We show in a paradigmatic case study that *structured losses* in the field can seed exotic emission properties. Photons can mediate dissipative, fully non-reciprocal interactions between emitters with range critically dependent on the loss rate. When this loss rate corresponds to a bare-lattice exceptional point, the effective couplings are exactly nearest neighbor, implementing a dissipative, fully non-reciprocal Hatano–Nelson model. Counterintuitively, this can occur irrespective of the lattice boundary conditions. Thus photons can mediate an effective emitter's Hamiltonian which is translationally invariant despite the fact that the field is not. We interpret these effects in terms of metastable atom–photon dressed states, which can be exactly localized on only two lattice cells or extended across the entire lattice. These findings introduce a paradigm of light-mediated interactions with unprecedented features such as non-reciprocity, non-trivial dependence on field boundary conditions, and range tunability via a loss rate.

https://doi.org/10.1364/OPTICA.443955

1. INTRODUCTION

The irreversible leakage of energy into an external reservoir is traditionally viewed as a detriment in physics, as losses usually spoil the visibility of several phenomena, in particular, those relying on quantum coherence. A longstanding tool for describing these detrimental effects is non-Hermitian (NH) Hamiltonians [1]. While their introduction dates back to the early age of quantum mechanics [2], only in recent years was it realized and experimentally confirmed that systems described by NH Hamiltonians can exhibit under suitable conditions a variety of exotic phenomena [3,4]. Among these are: coalescence of eigenstates at exceptional points (EPs) [5], unconventional geometric phase [6], failure of bulk-edge correspondence [7], critical behavior of quantum correlations around EPs [8–10], and NH skin effect [11]. As a typical consequence, traditional tenets of physics such as the Bloch theory of bands and even the very notion of "bulk" may require a non-trivial revision in the NH realm [12]. Such NH effects are intensively studied in several scenarios (such as mechanics, acoustics, electrical circuits, biological systems) [4] and, most notably, in view of our purposes here, optics and photonics [13,14].

Here, we investigate NH physics in a setup comprising a set of emitters (such as atoms, superconducting qubits, or resonators) coupled to a photonic lattice, implemented, e.g., by an array of coupled cavities [15–27]. Such types of systems are currently spurring considerable interest in the quantum optics community, in particular due to the possibility of tailoring directional emission [20,28,29] or exploiting photon-mediated interactions between emitters to engineer effective spin Hamiltonians [17,21,22,26,30]. Remarkably, the range and profile of these second-order interactions are directly inherited from the form of atom–photon dressed states (typically arising within photonic bandgaps), which in turn depend on the lattice *structure* [31]. Experimental implementations were demonstrated in various architectures such as circuit quantum electrodynamics (QED) [32–34], cold atoms coupled to photonic crystal waveguides [35], and optical lattices [36,37].

Studying the spoiling effect of photon leakage in such quantum optics setups is a routine task, even through NH Hamiltonians (see, e.g., Ref. [18]), the usual configuration considered being yet that of uniform losses. In contrast, here we introduce an engineered *pattern* of photonic losses so as to affect the photonic normal

modes. The basic question we ask is whether and to what extent shaping the field structure through patterned leakage (besides photonic hopping rates) can affect the nature of atom–photon interactions, and hence photon-mediated couplings.

By considering a paradigmatic case study, we will in particular show that photons can mediate dissipative non-reciprocal interactions between emitters with exotic features such as: (i) loss-dependent interaction range (from purely long range to purely nearest neighbor), (ii) formation of short- and long-range metastable dressed states, and (iii) insensitivity to the field boundary conditions (BCs).

2. SETUP AND HAMILTONIAN

The setup we consider [see Fig. 1(a)] comprises a composite 1D photonic lattice (coupled-cavity array), whose unit cell consists of a pair of cavities denoted with a and b.

Importantly, only cavities b are leaky, the associated loss rate being γ. By denoting with a_n (b_n), the bosonic annihilation operator of cavity a (b) in the nth cell, the bare Hamiltonian of the field reads (we set $\hbar = 1$ throughout)

$$H_f = \frac{J}{2}\sum_{n=1}^{N}\left[a_n^\dagger b_{n+1} + b_n^\dagger a_{n+1} - i a_n^\dagger a_{n+1} + i b_n^\dagger b_{n+1} + 2a_n^\dagger b_n + \text{H.c.}\right] - i\gamma\sum_{n=1}^{N} b_n^\dagger b_n, \tag{1}$$

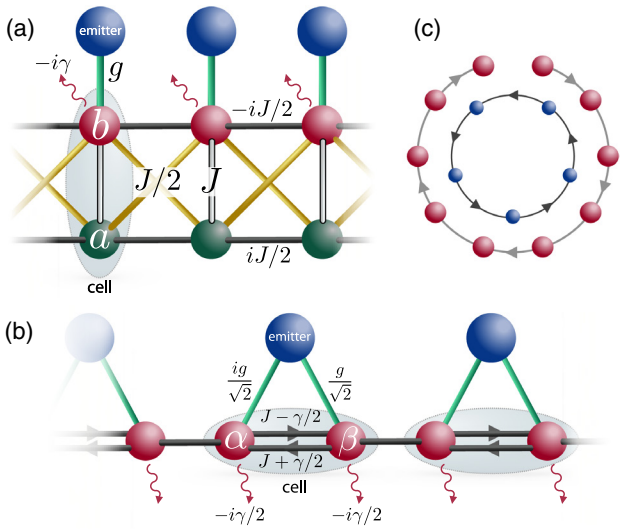

Fig. 1. (a) Setup: photonic lattice with unit cell comprising a pair of cavities labeled a (lossless) and b (lossy). Each quantum emitter is locally coupled to a lossy cavity. (b) Same setup as (a) defined by the unitary (intra-cell) transformation Eq. (3). All cavities are now lossy with uniform loss rate $\gamma/2$ while intra-cell couplings are non-reciprocal. The bare photonic lattice is a non-Hermitian generalization of the SSH model. Each emitter now couples to the lattice at *two* different sites whose respective couplings differ by a $\pi/2$ phase. (c) Schematics of the bare field Hamiltonian H_f (odd N) under open BCs (open loop) and the corresponding induced effective Hamiltonian of the emitters, H_{eff} (closed loop) for $N_e = N$, and $\gamma = 2J$. Both Hamiltonians feature fully non-reciprocal couplings but with opposite chirality, where H_{eff} in particular implements a dissipative Hatano–Nelson model. Remarkably, H_{eff} is translationally invariant despite the bare field (hence the total system) breaks translational invariance.

with N the numbers of lattice cells. The first line describes the interaction between neighboring cells, i.e., the $a-a$ and $b-b$ horizontal couplings and $a-b$ diagonal couplings with strength $J/2$ [see Fig. 1(a)]. In the second line, the first term describes the intra-cell interaction, i.e., the vertical $a-b$ couplings (strength J), whereas the last term accounts for the local losses on b cavities. Note that for $\gamma = 0$, we would have $H_f^\dagger = H_f$, namely, the NH nature of the field Hamiltonian comes only from the local losses on b cavities (the overall setup being passive). Model Eq. (1) is well known in the NH physics literature as the Lee model [7,38].

The system additionally comprises N_e identical two-level quantum emitters ("atoms"), each locally coupled under the rotating wave approximation to a lossy cavity b [see Fig. 1(a) showing the case $N_e = N$]. The total Hamiltonian is thus

$$H = H_f + \sum_{i=1}^{N_e} g(\sigma_i^\dagger b_{n_i} + b_{n_i}^\dagger \sigma_i), \tag{2}$$

with n_i the cavity directly coupled to the ith atom, and where $\sigma_i = |g\rangle_i\langle e|$ is the pseudo-spin ladder operator of the ith atom with $|g\rangle$ and $|e\rangle$, respectively, the ground and excited states.

We anticipate that the physical properties that we are going to focus on involve only a single excitation and are thus insensitive to the nature of the ladder operators σ_i of the emitters, which could thus be thought of as cavities/oscillators themselves [39,40]. Our system could thus be implemented as well in an all-photonic scenario.

In the above, we assumed that the cavities (either a or b) and emitters all have the same frequency ω_0 and set this to zero (i.e., energies are measured from ω_0).

A key feature of the bare photonic lattice [cf. Fig. 1(a) and Hamiltonian H_f] is that, for $\gamma \neq 0$, it is *non-reciprocal* in that photons propagate preferably from right to left. Thus losses endow the structure with an intrinsic left–right asymmetry. One can show that the complex $a-a$ couplings energetically favor left propagating photon and $b-b$ couplings favor right propagating ones. Indeed, under the standard Peierls substitution (see, e.g., Ref. [41]), the kinetic energy associated with a hopping term is minimized by the momentum $k = \theta$, where θ is the complex phase of the hopping amplitude, which is $\theta = -\pi/2$ for the $a-a$ couplings and $\theta = \pi/2$ for $b-b$ couplings. When losses are present (i.e., for $\gamma \neq 0$) the left–right symmetry is broken because right-propagating photons (lying predominantly on b sites) are more subject to dissipation than left-propagating ones. This effectively results in photons propagating leftwards with higher probability than rightwards.

Such a dissipation-induced non-reciprocity, which was shown also in other lattices (see, e.g., Ref. [42]), can be formally derived by performing the field transformation [38] $\{a_n, b_n\} \to \{\alpha_n, \beta_n\}$ with

$$a_n = \frac{1}{\sqrt{2}}(\alpha_n - i\beta_n), \qquad b_n = -\frac{i}{\sqrt{2}}(\alpha_n + i\beta_n). \tag{3}$$

This unitary, which is local in that it mixes cavity modes of the same cell, defines a new picture where the free field Hamiltonian now reads [see Fig. 1(b)]

$$H_f' = \sum_n\left[\left(J+\frac{\gamma}{2}\right)\alpha_n^\dagger\beta_n + \left(J-\frac{\gamma}{2}\right)\beta_n^\dagger\alpha_n\right] + \sum_n J(\alpha_{n+1}^\dagger\beta_n + \text{H.c.}) - i\frac{\gamma}{2}\sum_n(\alpha_n^\dagger\alpha_n + \beta_n^\dagger\beta_n). \tag{4}$$

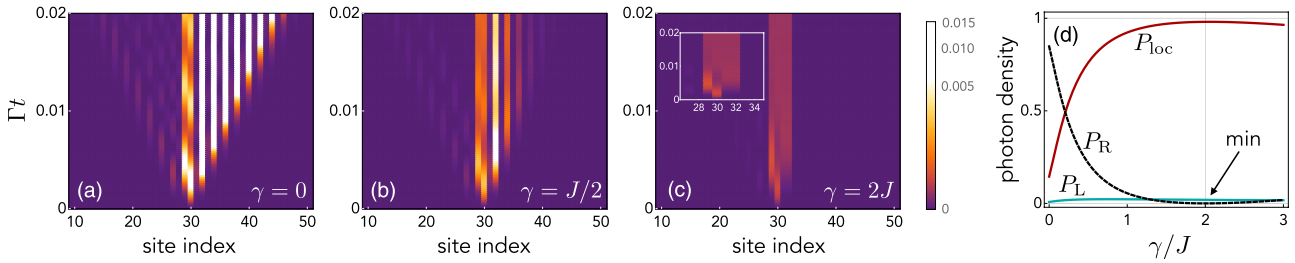

Fig. 2. Field dynamics during spontaneous emission. (a)–(c) Spatial profile of photon density $|\langle\eta_n||\Psi_t\rangle|^2$ versus time, where $|\Psi_t\rangle = e^{-iHt}|\Psi_0\rangle$, $|\eta_n\rangle = |g\rangle\eta_n^\dagger|\text{vac}\rangle$, $\eta = a, b$ [referring to the original picture of Fig. 1(a)]. In the plots, we re-indexed cavities in a way that neutral (lossy) cavities are labeled by odd (even) site indices. We set $g = 0.1J$ and $N = 100$ with the atom coupled to the lossy cavity of cell $n = 15$ [see Fig. 1(a)]. Time is measured in units of Γ^{-1} with $\Gamma = g^2/(4J)$. The atom's excited-state population $p_e = |\langle e|\langle\text{vac}||\Psi_t\rangle|^2$ decays exponentially as $p_e(t) = e^{-\Gamma t}$. (d) Functional dependence of P_{loc}, P_R, and P_L on the loss rate γ/J (where each probability is rescaled to the sum $P_L + P_{\text{loc}} + P_R$). Here, P_{loc} is the time-averaged probability to find the photon in the cell where the atom lies or the right nearest-neighbor cell (four cavities overall), while P_L (P_R) is the probability to find it in the remaining left (right) part of the lattice. We set an average time $t_{\text{av}} \sim 20J^{-1}$ with g small enough such that $t_{\text{av}} < \Gamma^{-1}$.

This tight-binding Hamiltonian is a NH generalization of the Su–Schrieffer–Heeger (SSH) model [38,43]. Unlike the original picture, H'_f features uniform loss on all cavities with rate $\gamma/2$. Remarkably, intra-cell couplings are now manifestly *non-reciprocal* for non-zero γ: the hopping rate of a photon from site α_n to β_n differs from that from β_n to α_n (respectively, $J + \frac{\gamma}{2}$ and $J - \frac{\gamma}{2}$). Inter-cell couplings J are instead reciprocal. We see that whenever $\gamma \neq 0$ [non-zero cavity leakage in the original picture; see Fig. 1(a)], the mapped lattice features an intrinsic chirality (i.e., non-reciprocity) in that the rate of photon hopping depends on the direction (rightward or leftward). At the critical value $\gamma = 2J$, which corresponds to an EP of the bare lattice [7], the intra-cell couplings are fully non-reciprocal (all couplings $\alpha_n \to \beta_n$ vanish). Thus at this EP, photons can propagate only to the left.

Consider now the *total* Hamiltonian in the new picture, which using Eq. (3) reads [cf. Eqs. (2) and (4)]

$$H' = H'_f + \sum_{i=1}^{N_e} \frac{g}{\sqrt{2}} \left(\sigma_i^\dagger(\beta_{n_i} - i\alpha_{n_i}) + \text{H.c.}\right). \tag{5}$$

Notably [see Fig. 1(b)], in the new picture, the atom–field interaction is no longer local, as each atom is coupled to *both* cavities α and β of the same cell. The corresponding (complex) couplings have the same strength but, importantly, a $\pi/2$ phase difference.

Thus, to sum up, in the picture defined by Eq. (3), the system features: (i) uniform losses, (ii) intra-cell non-reciprocal photon hopping rates, and (iii) bi-local emitter–lattice coupling. The simultaneous presence of these three factors is key to the occurrence of the phenomena to be presented.

3. SPONTANEOUS EMISSION OF ONE EMITTER

To begin with, we consider only one emitter ($N_e = 1$) and study spontaneous emission (initial joint state $|\Psi_0\rangle = |e\rangle|\text{vac}\rangle$ with $|\text{vac}\rangle$ the field's vacuum state), and we set $g \ll J$. When $\gamma = 0$ (no loss), the bare lattice is effectively equivalent to a standard tight-binding model with uniform nearest-neighbor couplings [see Fig. 1(b)] yielding a single frequency band of width $2J$ with the atom's frequency at its center.

Figures 2(a)–2(c) report the time behavior of the photon density profile across the lattice for different loss rates γ, while the atom's excited-state population decays exponentially as $p_e = e^{-\Gamma t}$ with $\Gamma = g^2/(4J)$ (not shown in the figure; see caption for details).

For $\gamma = 0$ (no loss), directional emission occurs in that the photon propagates predominantly to the right. This is a known effect [28] due to the effective bi-local coupling and $\pi/2$ phase difference in the picture in Fig. 1(b), which effectively suppresses the interaction of the emitter with left-going modes of the field. As γ is turned on (lattice leaky) the behavior considerably changes [see Figs. 2(b) and 2(c)]. Based on the previously discussed non-reciprocity of intra-cell couplings [see Fig. 1(b)], one might now expect the emitted photon to propagate away mostly to the left (in contrast to the $\gamma = 0$ case). Instead, this behavior is generally exhibited only by a tiny fraction of emitted light. Rather, a significant part *localizes* within a very narrow region of the lattice and eventually leaks out on a long time scale of the order of $\Gamma^{-1} \gg \gamma^{-1}$. Such photon localization dominates for $\gamma = 2J$ [see Fig. 1(c)], at which value it occurs strictly in two cells only: the one directly coupled to the atom and the nearest neighbor on the right. This is best illustrated in Fig. 2(d), where the time-averaged fraction of light localization in these two cells (P_{loc}) is plotted versus γ/J along with the fraction lying in the remaining left and right parts of the lattice (P_L and P_R, respectively). We note that P_{loc} is maximum at the EP, where $P_R = 0$ and $P_L \simeq 0$ (for $g \to 0$, $P_L \to 0$).

4. MANY EMITTERS

We consider next a pair of quantum emitters and study the (dissipative) dynamics of excitation transfer between them when one is initially excited and the other is in the ground state. We again set $\gamma = 2J$ [see Fig. 1(b)]; hence, the photonic lattice has an intrinsic *leftward* chirality.

When the atoms lie in nearest-neighbor cells [see Fig. 3(a)], an excitation initially on the left emitter is partially transferred to the right emitter with a characteristic rate $\sim\Gamma$ with both emitters eventually decaying to the ground state (transfer is only partial because of the leakage). Notably, as shown by Fig. 2(b), the reverse process does not occur: if the excitation now sits on the right emitter, this simply decays to the ground state with the left atom remaining unexcited all the time. Thus the field mediates a fully *non-reciprocal* (dissipative) interaction between emitters. At first sight, one might expect this second-order interaction to straightforwardly follow from the aforementioned intrinsic uni-directionality of the bare lattice [recall Fig. 2(b) for $\gamma = 2J$]. Yet, note that the directionality resulting from Figs. 3(a) and 3(b) is *rightward* in contrast to that of the lattice that, as said, is leftward [cf. Fig. 2(b)]. Later on, we will

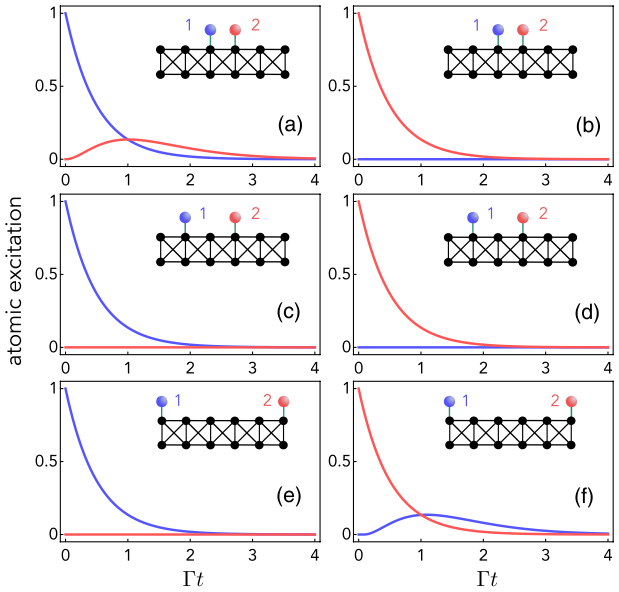

Fig. 3. Excitation transfer between two quantum emitters. We consider two quantum emitters ($N_e = 2$) and set $J = \gamma/2$. We plot the time behavior of emitter 1's excited-state probability p_1 (blue line) and that of emitter 2, p_2 (red) for the initial state $|\Psi_0\rangle = |e\rangle_1|g\rangle_2|\text{vac}\rangle$ [(a), (c), (e)] and $|\Psi_0\rangle = |g\rangle_1|e\rangle_2|\text{vac}\rangle$ [(b), (d), (f)], where $p_1 = |_1\langle e|_2\langle g|(\text{vac}|\Psi_t\rangle)|^2$ and an analogous definition holds for p_2. The inset in each panel shows the cells where the emitters sit in: nearest-neighbor cells [(a) and (b)], non-nearest-neighbor cells in the bulk [(c) and (d)], and edge cells [(e) and (f)]. We set $g = 0.1J$.

show that the lattice unidirectionality is indeed a key ingredient for such a non-reciprocal atomic cross talk, but, notably, not the only one.

Besides being non-reciprocal, the atom–atom effective interaction is *exactly* limited to emitters sitting in *nearest-neighbor* cells. This can be checked [see Figs. 3(c) and 3(d)] by placing the emitters in any pair of *non*-nearest-neighbor cells, in which case, no matter what atom is initially excited, no transfer occurs. A notable exception to this behavior yet arises when the lattice is open and emitters sit just on the two opposite edge cells. In this configuration [see Figs. 3(e) and 3(f)], counterintuitively, the coupling is again non-zero and fully non-reciprocal. The associated strength and directionality is just the same (up to a sign) as if the lattice were periodic and the two edge emitters were sitting next to each other [see Figs. 3(a) and 3(b)].

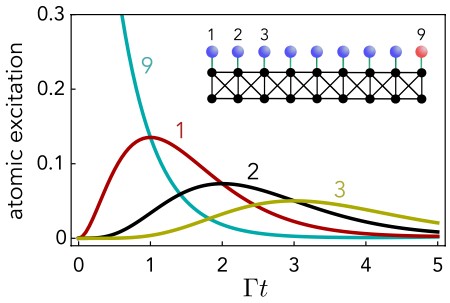

Fig. 4. Many-emitter excitation transfer. We set $N_e = N = 9$ (one emitter/cell) and plot against time the excited-state probability of atoms $n = 1$ (red line), $n = 2$ (black), $n = 3$ (yellow), and $n = 9$ (cyan) when atom $n = 9$ (sitting on the lattice right edge) is initially excited. We set $g = 0.1J$.

Results similar to those in Fig. 3 hold also for many emitters, in particular in the case of $N_e = N$ (one atom per unit cell). Figure 4 is the N-atom analog of Fig. 3(f): it clearly shows that an excitation initially on the Nth atom (on the right edge cell) is first transferred to atom 1 (sitting on the left edge), then atom 2, then 3, etc. Again, this behavior is compatible with nearest-neighbor non-reciprocal (rightward) effective couplings between the emitters where, remarkably, the emitters on the edges couple to one another as if the lattice were translationally invariant (ring). Indeed, it can be checked that plots in Fig. 4 remain identical if the lattice is now subject to periodic BCs (no edges).

5. EFFECTIVE HAMILTONIAN

All these dynamics (in particular) are well described by the effective Hamiltonian of the emitters, which for a bare lattice with periodic BCs reads

$$H_{\text{eff}} = \sum_{ij} \mathcal{H}_{n_i n_j} \sigma_i^\dagger \sigma_j \quad \text{with} \tag{6}$$

$$\mathcal{H}_{m\neq n} = i4g^2 J \frac{(\gamma - 2J)^{m-n-1}}{(\gamma + 2J)^{m-n+1}}, \qquad \mathcal{H}_{mm} = -i\frac{g^2}{\gamma + 2J}, \tag{7}$$

where periodic BCs are understood, i.e., in Eq. (7), any n is equivalent to $n + N$. Thus H_{eff} is *traslationally invariant*. This NH effective Hamiltonian can be derived analytically in the weak-coupling Markovian regime ($g \ll J$) through a natural NH generalization [39] of the standard resolvent method [1,44]. For $\gamma > 0$ and $N \gg \lambda$, where we defined the interaction range λ as

$$\lambda^{-1} = -\ln\left|\frac{\gamma - 2J}{\gamma + 2J}\right|, \tag{8}$$

the entries of $\mathcal{H}_{mn}$ above the main diagonal vanish (i.e., for $m < n$). Hence, inter-emitter couplings are non-reciprocal with rightward chirality for any $\gamma > 0$. Instead, the interaction range λ is strongly dependent on γ (see Fig. 5). For $\gamma = 0$ (no loss), λ diverges, witnessing that couplings are purely long range [see matrix plot in Fig. 5(b)]: all possible pairs of atoms are coupled with the same strength (in modulus) [28] [this can be checked from Eq. (7) for $\gamma \to 0$]. As γ increases, the interaction range decreases until vanishing at the lattice EP $\gamma = 2J$—where it exhibits a critical behavior (see cusp)—and then rises again as $\gamma > 2J$. The zero occurs because at $\gamma = 2J$ [cf. Eq. (7) for $\gamma \to 2J$], $\mathcal{H}_{m>n}$ is non-zero only for $m = n + 1$ where it takes the value $\mathcal{H}_{n+1,n} = ig^2/(4J) = i\Gamma \equiv \mathcal{H}_{1N}$ [see matrix plot in Fig. 5(c)]. At this point of the parameter space, therefore, besides being effectively periodic (see above) the non-reciprocal interaction between the emitters is exactly limited to nearest neighbors: this implements a Hatano–Nelson model [45] with fully non-reciprocal hopping rates and uniform on-site losses under periodic BCs. The results in Figs. 3 and 4 fully reflect these properties.

Even more remarkably and counterintuitively, it can be demonstrated [see Supplement 1, Section 3] that, for odd N, H_{eff} is *insensitive to the BCs* of the lattice (matching the results of Fig. 4). In other words, even if the lattice is subject to open BCs (ring with a missing cell), H_{eff} is always given by Eq. (6). For even N, the hopping rate across the missing cell is modified by just an extra minus sign [see Supplement 1, Section 3.C]. Figure 1(c) sketches the open lattice for $N_e = N$ (one atom/cell) and $\gamma = 2J$: both H_f and H_{eff} feature fully-non-reciprocal couplings yet with opposite

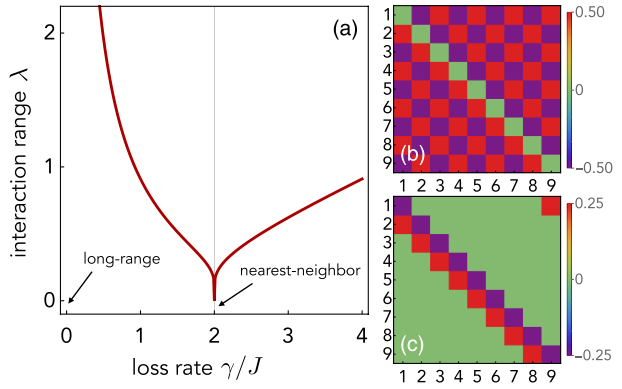

Fig. 5. Photon-mediated couplings between emitters. (a) Interaction range of H_{eff} (see main text) versus γ. (b), (c) Matrix plot of $\mathcal{H}_{mn}$ [cf. Eq. (7)] (imaginary part) for $\gamma = 0$ (b) and $\gamma = 2t_1$ (c) in units of g^2 (the real part vanishes). In (c), note the upper right corner witnessing that H_{eff} is translationally invariant. All plots are independent of the lattice boundary conditions.

chirality, and, moreover, H_{eff} is periodic while H_f is not. We thus, in particular, get that photons can mediate translationally invariant interactions between emitters despite the field (hence the total system) lacking translational invariance.

6. ATOM–PHOTON DRESSED STATE

Hamiltonian Eq. (6) can be understood in terms of a dressed atom–photon state $|\Psi\rangle$ mediating the second-order interaction between two generic emitters i and j according to the scheme: emitter $i \to |\Psi\rangle \to$ emitter j, where $|\Psi\rangle$ is a state where i is dressed by a single photon. The resulting i-j coupling is non-zero provided that $|\Psi\rangle$ has non-zero amplitude on the location of j [see Supplement 1, Section 3.D]. Similar descriptions were successfully applied to dissipationless interactions for lossless lattices with emitters inside bandgaps [17,20,22,26,29,46,47], in which case $|\Psi\rangle$ is stationary. In our lossy gapless lattice, instead, interactions between emitters are dissipative and $|\Psi\rangle$ metastable.

To pinpoint the essential physics, we set $\gamma = 2J$ (EP) and consider first an emitter sitting in any *bulk* cell indexed by $n = \nu$. It is convenient to refer to the picture in Fig. 1(b) and introduce a light notation such that $|e\rangle|\text{vac}\rangle \to |\text{e}\rangle$, while $|g\rangle|\eta_n\rangle \to |\eta_n\rangle$ with $\eta = \alpha, \beta$.

One can check by direct substitution that, to the second order in g/J, H admits the eigenstate and associated energy:

$$|\Psi\rangle = |e\rangle - i\tfrac{g}{\sqrt{2\gamma}}\left(|\beta_\nu\rangle - i|\alpha_{\nu+1}\rangle\right), \varepsilon = -i\Gamma \tag{9}$$

(recall that $\Gamma = g^2/4J$). Note that $|\Psi\rangle$ is normalized to the second order in g, while $|\Psi\rangle \to |e\rangle$ and for $g \to 0$. Most remarkably, $|\Psi\rangle$ is strictly localized in only two lattice cells (ν and $\nu+1$), in particular, on cavities β_ν and $\alpha_{\nu+1}$. Such strict localization is possible due to a simultaneous "decoupling" of $|\Psi\rangle$ from the lattice's right branch (sites $\beta_{\nu+1}, \alpha_{\nu+2}, \ldots$) and left branch ($\ldots, \beta_{\nu-1}, \alpha_\nu$). The right-branch decoupling requires $\langle\beta_{\nu+1}|H|\Psi\rangle = 0$ so that $|\Psi\rangle$ has a node on $\beta_{\nu+1}$, which is guaranteed by the non-reciprocal leftward nature of intra-cell hopping rates. To get the left-branch decoupling, instead, we must require $\langle\alpha_\nu|H|\Psi\rangle = 0$ (so that $|\Psi\rangle$ can have a node on α_ν). It is easily seen [see Supplement 1, Section 2] that this condition can be met only provided that $\varepsilon = -i\Gamma$ (showing the metastable nature of the state) plus,

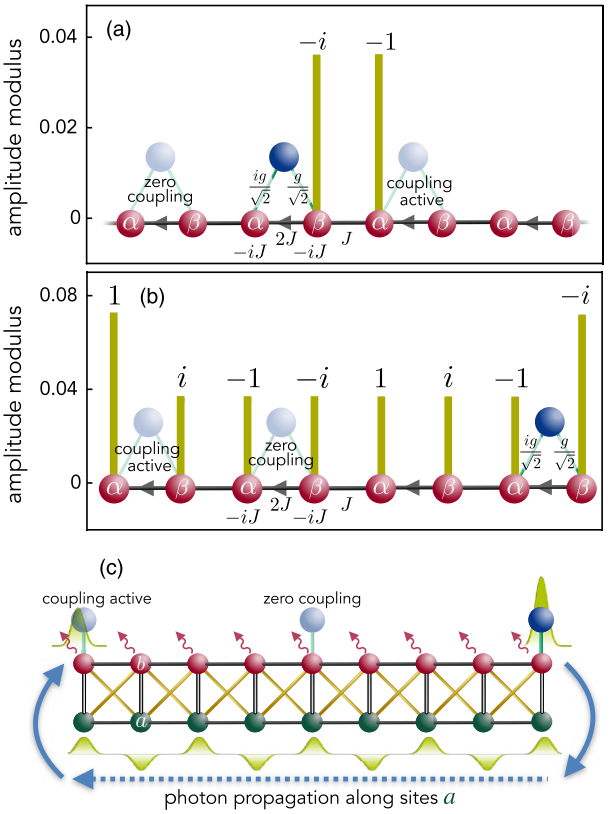

Fig. 6. Atom–photon dressed state mediating emitter–emitter interaction. (a) Dressed state $|\Psi\rangle$ forming when a quantum emitter ("source") is coupled to a bulk cell. Vertical bars measure the photonic wave function modulus. Another emitter (shaded) couples to $|\Psi\rangle$ ("coupling active"), hence to the source emitter, only provided that it sits in the right nearest-neighbor cell. If not ("zero coupling"), the two emitters do not interact. (b) Long-range dressed state arising when the source atom is coupled to the right-edge cell. Due to phase cancellation, an emitter placed in any bulk cell remains uncoupled from $|\Psi\rangle$ unless it lies on the opposite edge. In (a) and (b), we set $\gamma = 2J$ and refer to the picture in Fig. 1(b) defined by Eq. (3). (c) Pictorial representation of the state in (b) but in the original picture [cf. Fig. 1(a)]. Note that the photonic wave function is zero on all b sites in the bulk, which gives rise to a dissipationless channel bussing excitations between the two edges without involving emitters in the bulk.

crucially, $\langle\alpha_{\nu+1}|\Psi\rangle \neq 0$. The latter circumstance clarifies why the emitter can couple to another emitter sitting in cell $\nu+1$: any other location will give zero coupling since $|\Psi\rangle$ vanishes everywhere outside cells ν and $\nu+1$. This explains both the non-reciprocal and nearest-neighbor nature of H_{eff} at the lattice EP [cf. Eq. (6)] for atoms in the bulk.

We next consider an open lattice with the source atom now sitting in the cell on the right edge [see Fig. 6(b)]. Again by direct substitution, H can be shown to admit the eigenstate

$$|\Psi\rangle = |e\rangle - \frac{g}{\sqrt{2\gamma}}\sum_{n=1}^{N} e^{i\pi n}\left[(1+\delta_{n1})\,|\alpha_n\rangle - i\,(1+\delta_{nN})\,|\beta_n\rangle\right], \tag{10}$$

the associated energy still being $\epsilon = -i\Gamma$. This state is normalized to leading order in g under the condition $g \ll \gamma/\sqrt{N}$ [in line with the Markovian regime assumed to derive Eq. (6)]. Unlike Eq. (9), $|\Psi\rangle$ is extended across the entire lattice [see Fig. 6(b)]. In bulk sites, the photonic wave function has a flat modulus but non-uniform phase. Remarkably, the pattern of phases combines with

the bi-local nature of emitter–field coupling [see Figs. 1(b) and 6(b)] in such a way that, due to phase cancellation, another atom placed in any bulk cell cannot couple to $|\Psi\rangle$ (hence to the source atom). This conclusion yet does not apply to the leftmost cell, where $|\langle\alpha_1|\Psi\rangle| \neq |\langle\beta_1|\Psi\rangle|$: thus atoms placed on opposite edges are able to cross talk. For odd N, the resulting coupling strength matches that for nearest-neighbor emitters in the case of Fig. 6(a) [see Supplement 1, Section 3.C].

To better grasp the physical mechanism enabling Eq. (10) to mediate an interaction between edge emitters, it is useful to rewrite state Eq. (10) in the original picture [cf. Fig. 1(a)] through the inverse of Eq. (2). This reads

$$|\Psi\rangle = |e\rangle - \frac{g}{2\gamma}\sum_{n=1}^{N} e^{i\pi n}\left[(2+\delta_{1n}+\delta_{nN})|a_n\rangle + i(\delta_{1n}-\delta_{nN})|b_n\rangle\right]. \tag{11}$$

Note that the state has zero amplitude on all the lossy sites b in the lattice *bulk*. On one hand, this explains why state $|\Psi\rangle$ cannot mediate any cross talk between bulk atoms. On the other hand, it makes intuitive how the mediating photon can bus excitations between the system's edges without decaying in the bulk: as the unit cell contains a lossless site, there exists a dissipationless channel connecting the two lattice edges as sketched in Fig. 6(c).

Finally, we point out that the emergence of states Eqs. (9) and (10) relies on the simultaneous occurrence of properties (i)–(iii) at the end of Section 2, witnessing in particular the NH nature of the above physics.

7. DISCUSSION

These findings introduce a new quantum optics/photonics paradigm, where "structured" leakage on the field can shape unprecedented emission properties and second-order emitter–emitter dissipative interactions. Besides engineered leakage, a key ingredient for the predicted physics was shown to be the effectively non-local nature of emitter–field coupling (in a suitable picture). Emitters subject to such unconventional *non-local* interaction are dubbed "giant atoms" in the context of an emerging literature [48]. They can be implemented via superconducting qubits [49], cold atoms [50], or all-photonic setups [51] and seed tunable dipole–dipole Hamiltonians [30,52–54]. From such a perspective, the presented results stem from an interesting combination of giant atoms physics, NH Hamiltonians, and, in some respects, chiral quantum optics [55–57], holding the promise for further developments, e.g., using three-local coupling [58] and 2D NH lattices [59].

We point out that the considered setup [cf. Fig. 1] is fully passive. In our framework, this naturally follows from the decay nature of the studied phenomena, a type of non-unitary dynamics currently receiving considerable attention also in other scenarios [60]. On the other hand, the passive nature of our system favors an experimental verification of the predicted dynamics, e.g., in photonics (where NH Hamiltonians are often implemented through their passive counterparts [61]). A circuit-QED implementation appears viable as well: arrays of resonators coherently coupled to superconducting qubits—including excitation transfer mediated by atom–photon bound states—were experimentally demonstrated [33,34,62], and implementations of lattices like the one in Fig. 1(a) were put forward [63]. Patterned losses can be realized by interspersing resonators with low and high quality factors. This is easily achieved in state-of-the-art settings where external losses can be reduced up to four orders of magnitude compared to photon-hopping rates, while large losses can be obtained and controlled by selectively connecting lattice resonators to transmission lines [33,34,62].

It is natural to ask whether analogous effects occur also in photonic lattices different from the one considered here. We checked that this is the case for a sawtooth-like photonic lattice very similar to the one in Refs. [29,64] with added losses on one sublattice. A general classification of the photonic Hamiltonians exhibiting these physical properties is a desirable (and non-trivial) task that is left for future work.

Finally, whether by building on the physics presented here one could realize exotic interactions that are dissipationless (possibly adding active elements) is under ongoing investigation.

Funding. Ministero dell'Università e della Ricerca (PRIN project 2017SRNBRK QUSHIP); The Government of the Russian Federation (074-02-2018-330 (2)); H2020 Marie Skłodowska-Curie Actions (882536) project QUANLUX.

Acknowledgment. We acknowledge support from MUR through the PRIN Project. AC acknowledges support from the Government of the Russian Federation. GC acknowledges that results incorporated in this standard have received funding from the European Union Horizon 2020 research and innovation programme under the Marie Sklodowska-Curie for the project QUANLUX.

Disclosures. The authors declare no conflicts of interest.

Data availability. Data underlying the results presented in this paper are not publicly available at this time but may be obtained from the authors upon reasonable request.

Supplemental document. See Supplement 1 for supporting content.

REFERENCES

1. C. Cohen-Tannoudji, J. Dupont-Roc, G. Grynberg, and P. Thickstun, *Atom-Photon Interactions: Basic Processes and Applications* (Wiley Online Library, 1992, 2004).
2. G. Gamow, "Zur quantentheorie des atomkernes," Zeitschrift für Phys. **51**, 204–212 (1928).
3. R. El-Ganainy, K. G. Makris, M. Khajavikhan, Z. H. Musslimani, S. Rotter, and D. N. Christodoulides, "Non-Hermitian physics and PT symmetry," Nat. Phys. **14**, 11–19 (2018).
4. Y. Ashida, Z. Gong, and M. Ueda, "Non-Hermitian physics," Adv. Phys. **69**, 249–435 (2020).
5. M.-A. Miri and A. Alu, "Exceptional points in optics and photonics," Science **363**, eaar7709 (2019).
6. C. Dembowski, B. Dietz, H.-D. Gräf, H. L. Harney, A. Heine, W. D. Heiss, and A. Richter, "Encircling an exceptional point," Phys. Rev. E **69**, 056216 (2004).
7. T. E. Lee, "Anomalous edge state in a non-Hermitian lattice," Phys. Rev. Lett. **116**, 133903 (2016).
8. W. Cao, X. Lu, X. Meng, J. Sun, H. Shen, and Y. Xiao, "Reservoir-mediated quantum correlations in non-Hermitian optical system," Phys. Rev. Lett. **124**, 030401 (2020).
9. J. Huber, P. Kirton, S. Rotter, and P. Rabl, "Emergence of PT-symmetry breaking in open quantum systems," SciPost Phys. **9**, 052 (2020).
10. F. Roccati, S. Lorenzo, G. M. Palma, G. T. Landi, M. Brunelli, and F. Ciccarello, "Quantum correlations in PT-symmetric systems," Quantum Sci. Technol. **6**, 025005 (2021).
11. S. Yao and Z. Wang, "Edge states and topological invariants of non-Hermitian systems," Phys. Rev. Lett. **121**, 086803 (2018).
12. K. Yokomizo and S. Murakami, "Non-Bloch band theory of non-Hermitian systems," Phys. Rev. Lett. **123**, 066404 (2019).
13. L. Feng, R. El-Ganainy, and L. Ge, "Non-Hermitian photonics based on parity-time symmetry," Nat. Photonics **11**, 752–762 (2017).
14. S. Longhi, "Parity-time symmetry meets photonics: a new twist in non-Hermitian optics," Eur. Phys. Lett. **120**, 64001 (2017).
15. E. Shahmoon and G. Kurizki, "Nonradiative interaction and entanglement between distant atoms," Phys. Rev. A **87**, 033831 (2013).

16. F. Lombardo, F. Ciccarello, and G. M. Palma, "Photon localization versus population trapping in a coupled-cavity array," Phys. Rev. A **89**, 053826 (2014).
17. J. S. Douglas, H. Habibian, C. L. Hung, A. V. Gorshkov, H. J. Kimble, and D. E. Chang, "Quantum many-body models with cold atoms coupled to photonic crystals," Nat. Photonics **9**, 326–331 (2015).
18. G. Calajó, F. Ciccarello, D. Chang, and P. Rabl, "Atom-field dressed states in slow-light waveguide QED," Phys. Rev. A **93**, 033833 (2016).
19. T. Shi, Y.-H. Wu, A. González-Tudela, and J. I. Cirac, "Bound states in boson impurity models," Phys. Rev. X **6**, 021027 (2016).
20. A. González-Tudela and J. I. Cirac, "Quantum emitters in two-dimensional structured reservoirs in the nonperturbative regime," Phys. Rev. Lett. **119**, 143602 (2017).
21. A. González-Tudela and J. I. Cirac, "Markovian and non-Markovian dynamics of quantum emitters coupled to two-dimensional structured reservoirs," Phys. Rev. A **96**, 043811 (2017).
22. A. González-Tudela and J. I. Cirac, "Exotic quantum dynamics and purely long-range coherent interactions in Dirac conelike baths," Phys. Rev. A **97**, 043831 (2018).
23. A. González-Tudela and J. I. Cirac, "Non-Markovian quantum optics with three-dimensional state-dependent optical lattices," Quantum **2**, 97 (2018).
24. A. González-Tudela and F. Galve, "Anisotropic quantum emitter interactions in two-dimensional photonic-crystal baths," ACS Photon. **6**, 221–229 (2019).
25. E. Sánchez-Burillo, L. Martín-Moreno, J. J. García-Ripoll, and D. Zueco, "Single photons by quenching the vacuum," Phys. Rev. Lett. **123**, 013601 (2019).
26. L. Leonforte, A. Carollo, and F. Ciccarello, "Vacancy-like dressed states in topological waveguide QED," Phys. Rev. Lett. **126**, 063601 (2021).
27. D. De Bernardis, Z.-P. Cian, I. Carusotto, M. Hafezi, and P. Rabl, "Light-matter interactions in synthetic magnetic fields: Landau-photon polaritons," Phys. Rev. Lett. **126**, 103603 (2021).
28. T. Ramos, B. Vermersch, P. Hauke, H. Pichler, and P. Zoller, "Non-Markovian dynamics in chiral quantum networks with spins and photons," Phys. Rev. A **93**, 062104 (2016).
29. E. Sánchez-Burillo, C. Wan, D. Zueco, and A. González-Tudela, "Chiral quantum optics in photonic sawtooth lattices," Phys. Rev. Res. **2**, 023003 (2020).
30. X. Wang, T. Liu, A. F. Kockum, H.-R. Li, and F. Nori, "Tunable chiral bound states with giant atoms," Phys. Rev. Lett. **126**, 043602 (2021).
31. P. Lambropoulos, G. M. Nikolopoulos, T. R. Nielsen, and S. Bay, "Fundamental quantum optics in structured reservoirs," Rep. Prog. Phys. **63**, 455–503 (2000).
32. Y. Liu and A. A. Houck, "Quantum electrodynamics near a photonic bandgap," Nat. Phys. **13**, 48–52 (2017).
33. N. M. Sundaresan, R. Lundgren, G. Zhu, A. V. Gorshkov, and A. A. Houck, "Interacting qubit-photon bound states with superconducting circuits," Phys. Rev. X **9**, 011021 (2019).
34. M. Scigliuzzo, G. Calajò, F. Ciccarello, D. Perez Lozano, A. Bengtsson, P. Scarlino, A. Wallraff, P. Delsing, and S. Gasparinetti, "Probing nonlinear photon scattering with artificial atoms coupled to a slow-light waveguide," Bull. Am. Phys. Soc. (to be published).
35. J. D. Hood, A. Goban, A. Asenjo-Garcia, M. Lu, S.-P. Yu, E. Chang, and H. J. Kimble, "Atom–atom interactions around the band edge of a photonic crystal waveguide," Proc. Natl. Acad. Sci. USA **113**, 10507–10512 (2016).
36. L. Krinner, M. Stewart, A. Pazmiño, J. Kwon, and D. Schneble, "Spontaneous emission of matter waves from a tunable open quantum system," Nature **559**, 589–592 (2018).
37. M. Stewart, J. Kwon, A. Lanuza, and D. Schneble, "Dynamics of matter-wave quantum emitters in a structured vacuum," Phys. Rev. Res. **2**, 043307 (2020).
38. E. J. Bergholtz, J. C. Budich, and F. K. Kunst, "Exceptional topology of non-Hermitian systems," Rev. Mod. Phys. **93**, 015005 (2021).
39. S. Longhi, "Spectral singularities in a non-Hermitian Friedrichs-Fano-Anderson model," Phys. Rev. B **80**, 165125 (2009).
40. A. Crespi, F. V. Pepe, P. Facchi, F. Sciarrino, P. Mataloni, H. Nakazato, S. Pascazio, and R. Osellame, "Experimental investigation of quantum decay at short, intermediate, and long times via integrated photonics," Phys. Rev. Lett. **122**, 130401 (2019).
41. R. P. Feynman, R. B. Leighton, and M. Sands, *The Feynman Lectures on Physics*, New millennium ed. (Basic Books, 2010), Originally published 1963-1965.
42. S. Longhi, D. Gatti, and G. Della Valle, "Robust light transport in non-Hermitian photonic lattices," Sci. Rep. **5**, 13376 (2015).
43. W. P. Su, J. R. Schrieffer, and A. J. Heeger, "Solitons in polyacetylene," Phys. Rev. Lett. **42**, 1698 (1979).
44. E. Sánchez-Burillo, D. Porras, and A. González-Tudela, "Limits of photon-mediated interactions in one-dimensional photonic baths," Phys. Rev. A **102**, 013709 (2020).
45. N. Hatano and D. R. Nelson, "Localization transitions in non-hermitian quantum mechanics," Phys. Rev. Lett. **77**, 570–573 (1996).
46. A. González-Tudela, C. L. Hung, D. E. Chang, J. I. Cirac, and H. J. Kimble, "Subwavelength vacuum lattices and atom-atom interactions in two-dimensional photonic crystals," Nat. Photonics **9**, 320–325 (2015).
47. M. Bello, G. Platero, J. I. Cirac, and A. González-Tudela, "Unconventional quantum optics in topological waveguide QED," Sci. Adv. **5**, eaaw0297 (2019).
48. A. F. Kockum, "Quantum optics with giant atoms-the first five years," in *International Symposium on Mathematics, Quantum Theory, and Cryptography* (Springer, 2021), pp. 125–146.
49. M. V. Gustafsson, T. Aref, A. F. Kockum, M. K. Ekström, G. Johansson, and P. Delsing, "Propagating phonons coupled to an artificial atom," Science **346**, 207–211 (2014).
50. A. González-Tudela, C. S. Muñoz, and J. I. Cirac, "Engineering and harnessing giant atoms in high-dimensional baths: a proposal for implementation with cold atoms," Phys. Rev. Lett. **122**, 203603 (2019).
51. S. Longhi, "Photonic simulation of giant atom decay," Opt. Lett. **45**, 3017–3020 (2020).
52. A. F. Kockum, G. Johansson, and F. Nori, "Decoherence-free interaction between giant atoms in waveguide quantum electrodynamics," Phys. Rev. Lett. **120**, 140404 (2018).
53. B. Kannan, M. J. Ruckriegel, D. L. Campbell, A. F. Kockum, J. Braumüller, D. K. Kim, M. Kjaergaard, P. Krantz, A. Melville, B. M. Niedzielski, A. Vepsäläinen, R. Winik, J. L. Yoder, F. Nori, T. P. Orlando, S. Gustavsson, and W. D. Oliver, "Waveguide quantum electrodynamics with superconducting artificial giant atoms," Nature **583**, 775–779 (2020).
54. A. Carollo, D. Cilluffo, and F. Ciccarello, "Mechanism of decoherence-free coupling between giant atoms," Phys. Rev. Res. **2**, 043184 (2020).
55. R. Blatt and P. Zoller, "Quantum jumps in atomic systems," Eur. J. Phys. **9**, 250–256 (1988).
56. P. Lodahl, S. Mahmoodian, S. Stobbe, A. Rauschenbeutel, P. Schneeweiss, J. Volz, H. Pichler, and P. Zoller, "Chiral quantum optics," Nature **541**, 473–480 (2017).
57. D. Cilluffo, A. Carollo, S. Lorenzo, J. A. Gross, G. M. Palma, and F. Ciccarello, "Collisional picture of quantum optics with giant emitters," Phys. Rev. Res. **2**, 043070 (2020).
58. L. Guo, A. F. Kockum, F. Marquardt, and G. Johansson, "Oscillating bound states for a giant atom," Phys. Rev. Res. **2**, 043014 (2020).
59. M. Kremer, T. Biesenthal, L. J. Maczewsky, M. Heinrich, R. Thomale, and A. Szameit, "Demonstration of a two-dimensional PT-symmetric crystal," Nat. Commun. **10**, 435 (2019).
60. A. S. Sheremet, M. I. Petrov, I. V. Iorsh, A. V. Poshakinskiy, and A. N. Poddubny, "Waveguide quantum electrodynamics: collective radiance and photon-photon correlations," arXiv:2103.06824 (2021).
61. M. Ornigotti and A. Szameit, "Quasi PT-symmetry in passive photonic lattices," J. Opt. **16**, 065501 (2014).
62. E. Kim, X. Zhang, V. S. Ferreira, J. Banker, J. K. Iverson, A. Sipahigil, M. Bello, A. González-Tudela, M. Mirhosseini, and O. Painter, "Quantum electrodynamics in a topological waveguide," Phys. Rev. X **11**, 011015 (2021).
63. H. Alaeian, C. W. S. Chang, M. V. Moghaddam, C. M. Wilson, E. Solano, and E. Rico, "Creating lattice gauge potentials in circuit QED: the bosonic Creutz ladder," Phys. Rev. A **99**, 053834 (2019).
64. S. Lorenzo, S. Longhi, A. Cabot, R. Zambrini, and G. L. Giorgi, "Intermittent decoherence blockade in a chiral ring environment," Sci. Rep. **11**, 12834 (2021).